DOI: 10.1021/ma902679u

Macromolecules
ARTICLE

Welding Kinetics in a Miscible Blend of High-T_g and Low-T_g Polymers

Murat Guvendiren,[†] Rachel L. McSwain,[†] Thomas E. Mates,[‡] and Kenneth R. Shull*,[†]

[†]*Department of Materials Science and Engineering, Northwestern University, Evanston, Illinois 60208, and* [‡]*Materials Department, University of California, Santa Barbara, Santa Barbara, California 93106*

Received December 3, 2009; Revised Manuscript Received February 11, 2010

ABSTRACT: A model system consisting of poly(tetramethyl bisphenol A polycarbonate) (TMPC) and poly(ethylene oxide) (PEO) was used to study the adhesion between miscible blends of polymers with very different glass transition temperatures. Contact mechanics experiments were performed where identical miscible blend layers were held into contact and separated at elevated temperatures. These results were correlated with measurements of PEO diffusion using dynamic secondary ion mass spectrometry. For low PEO concentrations in the blend, adhesion was obtained above a critical temperature that was consistent with the Fox equation, but substantial adhesion was not obtained at any temperature for blends with higher PEO contents. The results indicate that adhesion requires sufficient mobility of the high-T_g TMPC component and can be enhanced by small additions of PEO. Larger additions of the highly mobile PEO lubricate the interface, eliminating the enhancement in adhesion that would otherwise result from diffusion of the high-T_g component across the interface.

Introduction

Considerable progress has been made in understanding the strength of the interface between immiscible polymer blends and on strategies that can be employed to strengthen these interfaces.[1−9] Studies of interfacial adhesion in miscible blend systems have focused primarily on the origins of fracture and adhesion in glassy polymers.[10−13] Studies involving semicrystalline polymers are generally more difficult to interpret because of the complex microstructure of semicrystalline polymers.[14−19] An interesting feature of the use of semicrystalline polymers is that mobility of the semicrystalline component and its ability to weld interfaces together is coupled to its melting temperature, T_m. For example, if a thin layer of semicrystalline polymer is placed between two glassy polymers with which it is miscible, the semicrystalline polymer can act as an adhesive layer that is able to weld the two glassy layers together. Because welding will only occur above T_m, the process can be postponed as long as necessary by keeping the samples below this temperature, even when the glass transition temperature, T_g, for the semicrystalline polymer is very low. As a result, the use of semicrystalline polymers provide a means for studying the effects of diffusion-mediated adhesion between polymers with very different glass transition temperatures.

In the experiments described in this paper we utilize a model system where poly(ethylene oxide) (PEO) is the low-T_g semicrystalline polymer and poly(tetramethyl bisphenol A polycarbonate) (TMPC) is the high-T_g, noncrystalline polymer. The relevant temperatures are T_m for PEO (∼65 °C), T_g for PEO (∼−60 °C),[20] and T_g for TMPC (∼190 °C).[21,22] The wide separation between the glass transition temperatures in this system enables us to study the role of the mobilities of the different blend components in the development of adhesion between these blends. The bulk characteristics of the TMPC/PEO blends were investigated by differential scanning calorimetry (DSC), and the diffusion of PEO in TMPC was characterized by dynamic secondary ion mass spectroscopy (DSIMS). Adhesion experiments were performed by bringing two layers of TMPC/PEO blends into contact with one another at a fixed temperature, maintaining contact at this temperature for different lengths of time, and separating the surfaces at this same temperature. This approach enabled us to independently study the effects of contact time and temperature. The experimental details are described in the following section, followed by a description of our results and a discussion of the adhesion mechanisms in this system.

*To whom correspondence should be addressed: e-mail k-shull@northwestern.edu.

Experimental Section

Materials and Sample Preparation. The PEO was synthesized previously by anionic polymerization and had a weight-average molecular weight (M_w) of 70 000 g/mol and a polydispersity of 1.07. The deuterated PEO used in the DSIMS experiments had a molecular weight of 90 000 g/mol. Cross-linked PDMS elastomer substrates were produced by using a Dow Corning Sylgard 184 silicone elastomer kit. For grafting purposes, polystyrene (PS) with a trimethoxysilyl end group was anionically polymerized previously with $M_w = 38\,000$ g/mol.

The sample geometry used in the adhesion experiments is shown in Figure 1a and consists of a rigid spherical glass indenter and an elastic substrate made from cross-linked PDMS. Figure 1b is a schematic representation of the molecular structure of the interface. The PDMS substrate was oxidized by exposure to UV/ozone for 30 min, with a Jelight Co. model 42 UVO-Cleaner. A thin layer of trimethoxsilyl end group PS was spun-cast onto the oxidized elastomer from a solution in toluene. In order to graft PS onto the oxidized PDMS surface, the sample was annealed for 1.5 h at 125 °C. The excess PS chains were removed by rinsing the surface in toluene. A layer of TMPC/PEO blend was spun-cast on a glass slide from a solution of warm toluene (60 °C) and then floated onto water. This film was then transferred onto the PS surface and annealed for 1.5 h at 120 °C, which effectively grafted the TMPC to the surface because of the miscibility of the TMPC and PS.[21] This same process is repeated for the hemispherical glass indenter. The compositions of TMPC/PEO blends used in the adhesion experiments were as follows: 100/0, 95/5, and 80/20, numbers indicating the wt % TMPC and wt % PEO, respectively.

 Published on Web 03/04/2010

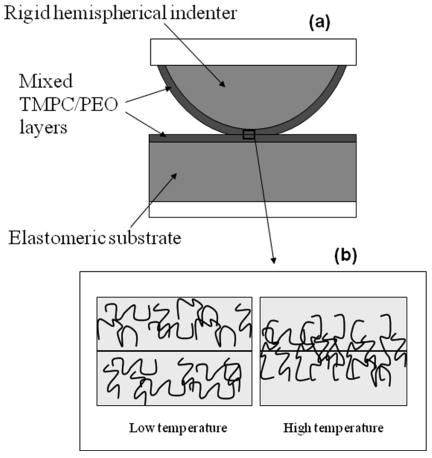

Figure 1. (a) Sample setup for adhesion testing of TMPC/PEO blends. (b) Schematic representation of the interface between two TMPC blends after contact at low and high temperatures.

Adhesion Tests. Adhesion experiments were conducted with a temperature-controlled axisymmetric indentation test method, which has been explained in detail previously.[19] In brief, the samples were mounted in a thermally insulated copper heating chamber, which was then connected to a 50 g load cell in series with a Burleigh inchworm stepping motor. The indenter was mounted to the lid of the heating chamber and aligned with the viewing window in the lid. This window allowed us to capture contact area images during the test from the reflected light microscope and camera mounted above the chamber. These images were then used to measure the radius of contact. The stepping motor advanced the elastomer substrate into and out of contact with the rigid indenter. A fiber-optic displacement sensor was placed below the sample holder to detect the displacement associated with the movement of the sample. A thermocouple, placed in the heating chamber in close proximity to the sample, was connected to a temperature controller so that the sample temperature can be controlled during the experiment.

To conduct the adhesion experiments, two different experimental protocols were utilized. In the first of these, which we refer to as protocol A, the system was first heated to a temperature of interest, which we refer as contact temperature, T_c, and the temperature was allowed to stabilize at $T_c \pm 3$ °C. The surfaces were then brought into contact at T_c and maintained in contact for a wide range of contact times $t_c = 0$, 10, 20, and 30 min. The surfaces were then pulled apart at T_c. Load and displacement data, and contact area images, were collected throughout each experiment. The actual times during which the surfaces were in contact were somewhat larger than t_c, since the contact time only refers to the hold time during which the displacement remained fixed. For the motor velocities used in our experiments (1 μm/s) the extra contact time corresponding to the loading and unloading portions of the experiment is a minute or less, which is generally much less than t_c.

The energy release rate, $\mathscr{G}$, defined as the energy available to propagate a crack along the interface, was calculated from the following expression:[23,24]

$$\mathscr{G} = \frac{((Ka^3/R) + P_t)^2}{6\pi K a^3} \tag{1}$$

where P_t is the tensile load, a is the contact radius, R is the radius of the curvature of the indenter (6 mm), and K is the modulus of elasticity. For an incompressible material with Poisson's ratio = 0.5, $K = 16E/9$, where E is the Young's modulus of the PDMS substrate. The modulus can also be obtained independently from the following relationship between the load and displacement, δ:[23,24]

$$\delta = \frac{a^2}{3R} + \frac{2P_t}{3Ka} \tag{2}$$

In this paper, we use a simple model to relate the measured load−displacement relationship to the relationship between the energy release rate and crack velocity. Our apparatus has a load cell in series with the sample and the motor used to control the displacement. The motor displacement, δ_m, is equal to the sum of δ and δ_s, where δ_s is the displacement of the spring in the load cell:[25,26]

$$\delta_m = \delta_s + \delta = \frac{P}{K_s} + \left(\frac{a^2}{3R} + \frac{2P}{3Ka}\right) \tag{3}$$

where K_s is the spring constant of the load cell. The contact perimeter can be viewed as a crack having a velocity, v, which is equal to the rate of change of the contact radius, i.e., $v = -(da/dt)$. The following form of the relationship between $\mathscr{G}$ and v has been found to describe a variety of contact problems involving elastomeric materials:[27,28]

$$\mathscr{G} = \mathscr{G}_c\left[1 + \left(\frac{v}{v^*}\right)^n\right] \tag{4}$$

Here $\mathscr{G}_c$ is the threshold adhesion energy, v^* is a characteristic crack velocity, and n is the exponent that defines the shape of the relationship between $\mathscr{G}$ and v. In our experiments the motor moves at a fixed rate, and we fit the resultant relationship between load and displacement using eqs 1−4, using $\mathscr{G}_c$, v^*, and n as adjustable parameters. The procedure is similar to that developed originally by Barquins and Maugis.[29]

The analysis procedure outlined above provides the most quantitative analysis of the data but is somewhat cumbersome for analyzing the relationship between the contact temperature and the adhesion that is obtained between the blend layers. For this purpose we also used a second procedure, which we refer to as protocol B. In these experiments the layers were brought into contact at room temperature, and the system was heated to the temperature of interest while the layers were already in contact. A total contact time of 20 min was used, during which the load remained fixed at 30 mN. Heating to the target temperature was complete within the first 10 min of this contact time and remained stable to within 3 °C during the rest of the experiment. A tensile displacement was then applied using a motor velocity of 1 μm/s until failure occurred. Approximate values for $\mathscr{G}_c$ were obtained from eq 1, using the maximum tensile load prior to failure for P_t and the contact radius during the hold time for a.

Differential Scanning Calorimetry (DSC). DSC experiments were performed on a Mettler Toledo DSC 822 under a dry nitrogen atmosphere. The solutions of TMPC/PEO blends, concentrations of 90/10, 80/20, 70/30, 60/40, 50/50, and pure PEO (0/100) (numbers representing the relative wt. percent of components in the blend), were made in warm toluene. The aluminum DSC pans were placed on a heated surface, and the solution was added dropwise to the pan to allow evaporation of the toluene without crystallization of the PEO. Once the toluene evaporated, the pan was removed from the heat and sealed. Prior to data collection the samples were heated from room temperature to 215 °C and held for 10 min to remove any thermal history. Data were collected as the sample was cooled at a rate of 10 K/min from 215 to −85 °C, held for 5 min, and then heated back to 215 °C at a rate of 10 K/min.

Dynamic Secondary Ion Mass Spectrometry (DSIMS). In order to obtain a depth profile of the diffusion of PEO into TMPC, dynamic SIMS experiments were performed on a Physical Electronics 6650 DSIMS instrument. In these studies,

the sample surface was bombarded with a 250 nA, 4 kV O^{2+} primary ion beam, which had a profiling rate of 0.28 nm/s and a beam diameter of ~40 μm. Negatively charged secondary ions were detected from the center 15% of the etched crater area by mass spectrometry. To detect the movement of the PEO chains, a deuterated form of the PEO, with a molecular weight of 90 000 g/mol, was used, and tests were run on a number of samples with different annealing temperatures. In these studies, samples were made by creating a double layer with deuterated PEO (dPEO) and TMPC. dPEO was directly spun-cast onto the Si substrate, forming a layer with a thickness of 7 nm. A layer of TMPC (242 nm) was spun-cast onto glass and floated on top of the dPEO layer.

SIMS analysis of polymer layers spun-cast onto silicon was difficult due to charging of the sample. To correct for this issue, a 600 eV defocused electron beam was used for charge compensation. To offset any mismatch in conductivity at the interface, a layer of oxide was also grown on the surface of the silicon before spin-coating with the polymers to provide an insulating layer. Substrate preparation involved rinsing the ⟨100⟩ silicon in a 49% hydrofluoric acid (HF) solution to remove the native oxide layer from the surface. After exposure to HF, the samples were rinsed three times in deionized water, followed by isopropanol, and then dried with nitrogen gas. A layer of oxide was grown on the silicon surface by heat treatment according to the specifications of the Massoud model,[30] which is based on the model for thermal oxidation of silicon proposed by Deal and Grove.[31] The silicon samples were heated to 950 °C for 2 h, which results in an oxide layer thickness of 52 nm.

Concentration profiles of dPEO were obtained initially as a plot of secondary ion yield as a function of time. The time is associated with the thickness of the sample, since the secondary ions are collected as the primary ion beam slowly etches the film. Therefore, the time is correlated to the thickness through independent measurements of the thicknesses of the polymer films. Conversion of the counts collected throughout the depth of the sample to the volume fraction of dPEO at these depths is obtained from the requirement that integration of the dPEO volume fraction profile must give the thickness of the originally spun-cast dPEO layer.

Results

Thermal Analysis. The cooling and heating curves obtained from DSC measurements for pure PEO and TMPC/PEO blends are shown in Figure 2. The labels for each curve represent the relative weight fractions of TMPC and PEO for the blend. The pure PEO sample (0/100) shows an endothermic melting peak at 66 °C during heating. This peak broadens as the TMPC concentration increases and disappears when the TMPC concentration reaches 90% (90/10 blend). Similar behavior is also observed for the cooling curves. These results indicate that PEO and TMPC are miscible and that PEO molecules do not have enough mobility to crystallize for TMPC/PEO blends having PEO concentrations less than 10%. Similar results have been reported for miscible blends such as poly(acetoxystrene)/PEO.[20] The miscibility of PEO and TMPC is consistent with the observed miscibility of PEO with bisphenol A polycarbonate (PC),[32−34] which has a similar molecular structure to TMPC.

The mobility of each component is determined by the proximity to an effective glass transition temperature for each component in the blend. Because chain connectivity constrains the local volume fraction surrounding a given blend component to be enriched in that component, the effective glass transition temperatures of the different blend components will not necessarily be equal to one another.[35] Lodge and McLeish have developed a useful qualitative

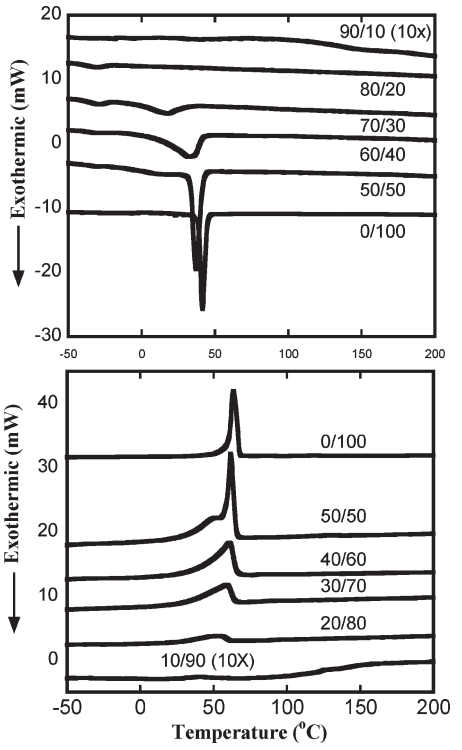

Figure 2. DSC cooling curves (top) and heating curves (bottom) for mixtures of TMPC and PEO. The labels on each curve correspond to the blend composition (TMPC volume percent/PEO weight percent).

formalism, based on the idea of a "self-concentration", that can be applied to our system.[36] The effective glass transition for component A is obtained by writing an equation similar to the Fox equation,[37] but where the actual volume fraction of component A is replaced by an effective volume fraction, ϕ_{effA}:

$$T_{\mathrm{gA}}^{\mathrm{eff}} = \left(\frac{\phi_{\mathrm{effA}}}{T_{\mathrm{gA}}} + \frac{1-\phi_{\mathrm{effA}}}{T_{\mathrm{gB}}} \right)^{-1} \tag{5}$$

where T_{gA} and T_{gB} are the glass transition temperatures of the pure components. The effective volume fraction for component is dependent on the local volume fraction and has a minimum value (for a very dilute solution of A in B) that is given by the self-concentration of component A, ϕ_{sA}:[36]

$$\phi_{\mathrm{effA}} = \phi_{\mathrm{sA}} + (1-\phi_{\mathrm{sA}})\phi_{\mathrm{A}} \tag{6}$$

where ϕ_{A} is the average global volume fraction of A in the sample. The self-concentration of A is the average local volume fraction of A around a given segment, averaged over a relatively small length scale (in the nanometer range) that governs the local segmental dynamics. The effective glass transition temperature for component B is obtained from equations that are exactly analogous to eqs 5 and 6, but with the A subscripts replaced by B.

Calculated effective glass transition temperatures for PEO and TMPC are plotted as the dashed lines in Figure 3 for the relatively low PEO volume fractions that are most relevant to our adhesion measurements. For these calculations we have assumed a self-concentration of 0.4 for both components, values that are consistent with previous experimentally determined values.[35] The solid line in Figure 3 is the prediction of the Fox equation,[37] which is the limiting form

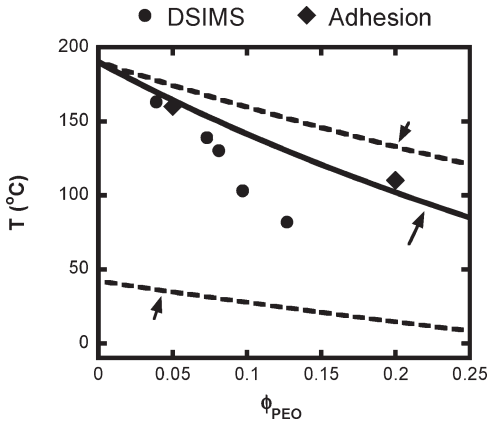

Figure 3. Concentration dependence of different characteristic temperatures obtained from the DSIMS and adhesion measurements (symbols). Solid and dashed lines represent the predictions of eq 5 and 6, with the indicated values of the self-concentrations.

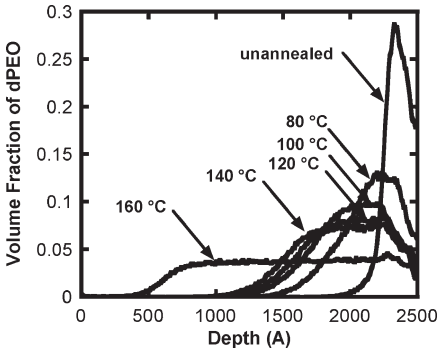

Figure 4. dPEO depth distributions for an unannealed sample and for samples annealed at the indicated temperatures for 1 h.

obtained by setting the self-concentrations equal to 0. At these relatively low PEO volume fractions, the assumed values for the self-concentrations do not substantially affect the predicted effective glass transition temperatures of the TMPC. The PEO effective glass transition is substantially affected, however. At a PEO volume fraction of 20%, for example, the bulk melting temperature for PEO is well into the glassy regime according to the Fox equation but is well above T_{gPEO}^{eff} if a self-concentration of 0.4 is assumed. The observed ability of the PEO to crystallize at comparable concentrations is therefore inconsistent with a self-concentration of zero but quite consistent with a self-concentration of 0.4. These results are also consistent with the effective glass transition temperatures obtained for miscible PS/TMPC blends reported by Kim et al.[21]

PEO/TMPC Interdiffusion. The concept of an effective glass transition of the PEO segments provides a framework for understanding the DSIMS results, which were designed to probe the interdiffusion of dPEO and TMPC. dPEO volume fraction profiles for an unannealed sample and for samples annealed at different temperatures for 1 h are shown in Figure 4. These samples had a 70 Å bottom layer of dPEO and a 2420 Å top layer of TMPC. The width of the dPEO layer of the unannealed sample is indicative of the depth resolution of the technique. The annealed samples all-show non-Fickian volume fraction profiles with a plateau value of the PEO concentration that decreases as the annealing temperature is increased. The volume fraction profiles are similar to case II diffusion fronts observed when low-T_g materials (either a low-molecular-weight solvent or low-T_g polymer) diffuse into a polymer with a glass transition temperature above the annealing temperature.[38,39] In our case the PEO diffusion coefficient in the PEO-rich region is much larger than the diffusion coefficient in the region that has not yet been swollen by PEO. As a result, the time required for the PEO to diffuse across the entire PEO-rich region is small in comparison to the time required for this region to expand further into the TMPC-rich phase.

The plateau value of the PEO concentration in the PEO-rich phase is a kinetically controlled parameter that provides some additional insight into the effective glass transition temperature of the PEO component. The mobility of the PEO must be high enough so that a swelling pressure is exerted on the TMPC-rich portion of the film, moving the boundary between the PEO-rich and TMPC-rich portions to lower depths and decreasing the plateau value of the PEO volume fraction in the PEO-rich layer. The process is self-limiting because the mobility of the PEO decreases as the local volume fraction of PEO decreases. As the effective glass transition of the PEO-rich portion of the film approaches the annealing temperature, the plateau concentration will no longer evolve. For this reason the annealing temperature serves as an upper bound to the effective glass transition temperature of a blend with a composition equal to the observed plateau concentration in the PEO-rich portion of the film. It is an upper bound to this quantity because other factors apart from PEO mobility in the PEO-rich portion will affect the swelling of the underlying TMPC-rich layer in ways that are difficult to predict.

The solid circles in Figure 3 represent the combinations of annealing temperature and plateau PEO concentrations obtained from the DSIMS experiments. The annealing temperatures are above the values of T_{gPEO}^{eff} obtained from the assumption that the PEO self-concentration is 0.4, a result that is consistent with the annealing temperature as an upper bound for T_{gPEO}^{eff}. More significantly, the annealing temperatures for the larger PEO fractions are much lower than the values corresponding to the Fox equation, for which the PEO self-concentration is zero. These results provide additional evidence that the self-concentration effect is needed in order to account for the mobility of the PEO segments.

Adhesion. If two TMPC/PEO blends are brought into contact with one another at temperatures that are high enough so that the PEO molecules can diffuse across the interface and provide a mechanical coupling between the two sides (Figure 1b), one expects that the presence of these linking molecules will affect the adhesion between the two blend layers. In order to study this diffusion-mediated adhesion process, axisymmetric pull-off tests were performed on thin layers of TMPC/PEO blends at elevated temperatures. A glass indenter and an elastomer substrate, both with adhered thin layers of TMPC/PEO blends, were brought into contact at an elevated temperature, T_c. The surfaces were pulled apart at this same temperature after the contact was maintained for different amounts of contact time, t_c, ranging from 0 to 30 min. A typical load vs displacement plot is shown in Figure 5, which corresponds to two 80/20 blends that were brought into contact at 100 °C and pulled apart after a contact time of 30 min. The solid curve represents the experimental data, and the open circles represent the fit obtained from the procedure outlined in the Experimental Section. For the empirical fits, the data were obtained by changing the threshold energy, $\mathcal{G}_c$, for fixed values of $v^* = 0.01$ μm/s and $n = 0.02$. The relationship between $\mathcal{G}$ and the contact radius obtained from this procedure is shown in Figure 6 for a range of contact times. As the surfaces are pulled apart, a stays constant for values

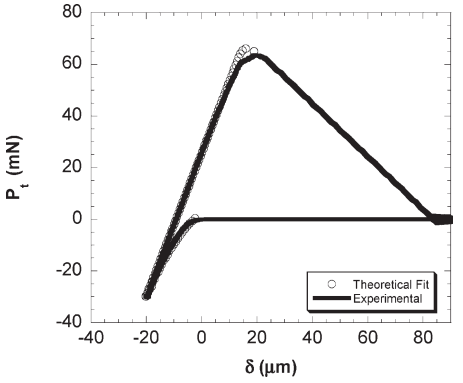

Figure 5. Tensile load−displacement data for the contact of two 80/20 (TMPC/PEO) thin film blends at 100 °C. The surfaces were brought into contact and held for 30 min at a compressive load of 30 mN. The solid line represents experimental data, and the circle represents theoretical fit using the procedure outlined in the Experimental Section.

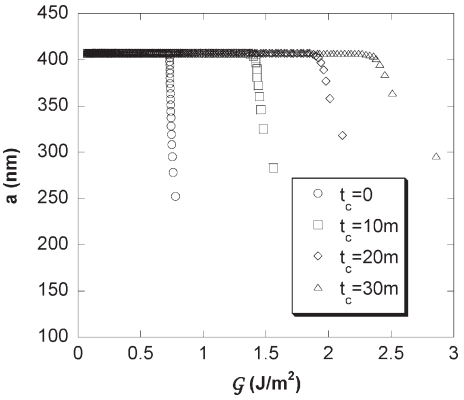

Figure 6. Relationship between contact radius and applied energy release rate for 80/20 (TMPC/PEO) blends at 100 °C. Data for contact times of 0, 10, 20, and 30 min are included.

of $\mathcal{G} < \mathcal{G}_c$. When $\mathcal{G}$ approaches $\mathcal{G}_c$, the crack starts moving and the contact radius decreases. At 100 °C, the threshold energy increases with an increase in contact time. This result is consistent with a welding process that is mediated by diffusive motions of molecules across the interface.

In order to investigate the temperature dependence of the diffusive processes responsible for adhesion between the TMPC/PEO blends, two different types of experiments were performed. The first of these involved duplication of the experiment outlined above (referred to as protocol A in the Experimental Section), but with a variety of contact temperatures. In addition to experiments corresponding to Figures 5 and 6, which were performed at 100 °C, identical experiments were performed at 25, 50, and 80 °C. From each of these experiments we obtain the relationship between contact time, t_c and the threshold energy release rate, $\mathcal{G}_c$. The results of these experiments for each of the temperatures studied are shown in Figure 7, where $\mathcal{G}_c$ is plotted as a function of t_c. These experiments indicate that, for the 80/20 TMPC/PEO blends, substantial adhesion is obtained only when the contact temperature reaches 100 °C.

A more complete picture of the effect of contact temperature for different blend compositions is obtained by heating layers in contact to different temperatures and then separating the surfaces at the elevated temperature until failure occurs (protocol B in the Experimental Section). In addition to the slight difference in experimental procedure, a simpler method is used to estimate $\mathcal{G}_c$, where the maximum tensile

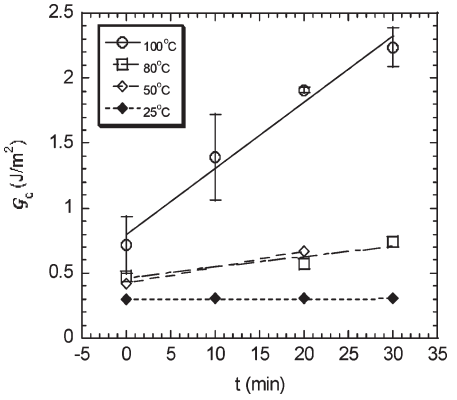

Figure 7. Threshold values of the energy release rate as a function of contact time for 80/20 (TMPC/PEO) blends at different contact temperatures.

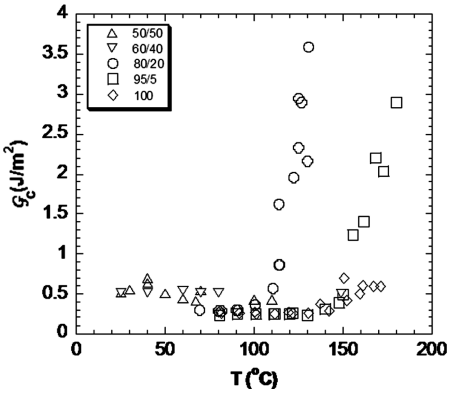

Figure 8. Threshold energy release rate as a function of contact temperature for different blends.

load and contact radius are substituted into eq 1, with the resultant value of $\mathcal{G}$ providing a good estimate for $\mathcal{G}_c$. Because of the detailed mechanics of our fracture geometry, this procedure provides an accurate measure of $\mathcal{G}_c$. For example, the procedure used in protocol A gives $\mathcal{G}_c = 2.1$ J/m^2 for the data in Figure 5, and the more simplified procedure of protocol B gives $\mathcal{G}_c = 2.3$ J/m^2. Values for the temperature dependence of $\mathcal{G}_c$ determined in this way for five different layer compositions are shown in Figure 8. Substantial adhesion is obtained only for blends with either 5 or 20 wt % PEO, and then only when the temperature is above some critical value. These critical temperatures are ∼160 °C for the 95/5 TMPC/PEO blend and ∼110 °C for the 80/20 TMPC/PEO blend and are included as diamonds in Figure 3. For the 80/20 blend the critical temperature is slightly higher than the critical temperature that would be expected based on the results plotted in Figure 7. While we do not have a definitive explanation for this difference, one possibility is that residual thermal stresses play a role in the experiments using protocol A (Figure 8), where the sample is brought to an elevated temperature while the samples are in contact.

Discussion

At this point we can use the data in Figures 3 and 8 to connect the adhesive response to a molecular-scale picture of the interface for different annealing temperatures. This picture must be consistent with the following observed features: (1) Welding of the blends surfaces to one another requires that the annealing temperature be above a critical value that is consistent with the

Fox equation (compare diamonds and solid line in Figure 3). (2) The critical temperature for interfacial welding is larger than the temperature required for substantial diffusion of PEO (compare diamonds to circles in Figure 3). (3) Substantial adhesion is not obtained at any temperature for PEO contents above 40% (from data in Figure 8).

Two limiting models of the role of the PEO molecules on the adhesive properties of the blends can be invoked to explain these results. We refer to these models as the "bridging" and "plasticization" models. In the bridging model mixing of TMPC segments across the interface does not occur, and the adhesion is mediated by the PEO molecules that bridge the interface. In the plasticization model, the PEO molecules plasticize the TMPC layer, enabling the TMPC molecules to mix across the interface. A definitive assessment of these limiting models is not possible because we do not have independent data for the mobility of TMPC molecules in the blends. Some important general comments can still be made, however. First, the distinction in component mobilities that is implicit in the bridging model does not appear to be valid for low PEO concentrations. For a PEO weight fraction of 0.05 the DSIMS data show that diffusive mobility of the PEO is attained at temperatures that are consistent with the Fox equation. These temperatures are more than 100 °C larger than the values obtained for values of the self-concentration that are used to understand glass transition data. This discrepancy is not necessarily surprising, since the self-concentration idea was developed to describe local segmental dynamics, whereas the DSIMS experiments are sensitive to diffusive motions over larger length scales.

For larger PEO volume fractions, the concept of a self-concentration becomes more consistent with the data on PEO diffusion, as the temperature required for PEO diffusion drops much more rapidly with PEO concentration than one would expect, based on an admittedly simplistic application of the Fox equation. Adhesion, however, is only observed at temperatures that are much higher than those required for PEO diffusion. This is evident by the critical temperature of adhesion of the blend with a PEO weight fraction of 0.2, which is again consistent with the Fox equation. For both of these blends the mobility of the TMPC component must itself play an important role in the development of adhesion, a result that is consistent with the plasticization model.

While some mixing of both PEO and TMPC segments appears to be a necessary condition for the welding of the surfaces in our experiments, this mixing does not guarantee that substantial adhesion is actually observed with the protocols that we employ. In our experiments the blend layers are separated at the same elevated temperature at which the welding takes place. If the interface is sufficiently mobile on the time scale of the debonding experiment, it might be possible for molecules to be pulled out across the interface so that only minimal adhesion is observed. This appears to be the case for the blends with PEO weight fractions above 0.4. At low temperatures there is not sufficient mobility of the TMPC molecules to form an adhesive interface. At higher temperatures the PEO molecules, present at substantial volume fractions, are so mobile that a strong interface cannot be maintained. If the samples are cooled after interdiffusion has taken place, the mobility of the PEO molecules is greatly diminished, and substantial adhesion is observed.[19] In these previous experiments a thin layer of PEO was spun-cast directly onto a pure TMPC layer, which was subsequently heated while in contact with a second TMPC layer. When these samples were cooled to room temperature prior to performing the adhesion measurement, very strong adhesion (sufficient to rupture the PDMS substrate) was observed in all cases. Overall, we find that the plasticization model provides an adequate explanation for all of these results. The presence of a substantial fraction of PEO chains with a temperature-dependent mobility provides a mechanism for interfacial failure and must also be taken into account when considering the overall effect on the interlayer adhesion.

Summary

We have studied the diffusion-mediated adhesion between two-component miscible polymer blends, with components that have component glass transition temperatures differing by 250 °C. The bulk properties of the blends were characterized by using DSC and dynamic SIMS, and the contact mechanics approach was utilized to study the self-adhesion of the blends. Our experiments have led to two important qualitative conclusions. The first of these is that the mobility of the dPEO in the blends decreases as the dPEO concentration decreases, with a temperature dependence that is much steeper than that given by the Fox equation. Our second conclusion is that adhesion requires sufficient segmental mobility of the high-T_g TMPC component so that some mixing of this component across the interface can occur. For volume fractions of PEO (up to 0.2) the critical temperature at which this mixing occurs is consistent with the Fox equation for the blend glass transition temperature. In this regime the added PEO enhances adhesion between the phases by plasticizing the interface and reducing the temperature that must be reached in order for this mixing to occur. If too much PEO is added (volume fractions exceeding 0.4), the interfacial dynamics are dominated by the fast-moving PEO chains, and minimal adhesion between the blend surfaces is observed at all temperatures, including those that are high enough to result in diffusion of the TMPC molecules across the interface.

Acknowledgment. This work was supported by the MRSEC program of the National Science Foundation (DMR-0076097) at the Materials Science Research Center of Northwestern University. The SIMS facility at the University of California at Santa Barbara is a facility of the MRL, also supported by the NSF MRSEC program (DMR05-20415). We thank Mark Hammersky of Proctor and Gamble for providing the TMPC used in these experiments. We also thank Nathan Yoder from Prof. Mark Hersam's research group at Northwestern University for assistance with the HF treatment of silicon wafers used in the SIMS experiments.

References and Notes

(1) Brown, H. R.; Char, K.; Deline, V. R.; Green, P. F. *Macromolecules* **1993**, *26*, 4155.
(2) Char, K.; Brown, H. R.; Deline, V. R. *Macromolecules* **1993**, *26*, 4164.
(3) Cho, K.; Brown, H. R.; Miller, D. C. *J. Polym. Sci., Part B: Polym. Phys.* **1990**, *28*, 1699.
(4) Creton, C.; Kramer, E. J.; Hui, C. Y.; Brown, H. R. *Macromolecules* **1992**, *25*, 3075.
(5) Creton, C.; Brown, H. R.; Deline, V. R. *Macromolecules* **1994**, *27*, 1774.
(6) Kulasekere, R.; Kaiser, H.; Ankner, J. F.; Russell, T. P.; Brown, H. R.; Hawker, C. J.; Mayes, A. M. *Macromolecules* **1996**, *29*, 5493.
(7) Shull, K. R.; Kramer, E. J.; Hadziioannou, G.; Tang, W. *Macromolecules* **1990**, *23*, 4780.
(8) Washiyama, J.; Kramer, E. J.; Hui, C. Y. *Macromolecules* **1993**, *26*, 2928.
(9) Willett, J. L.; Wool, R. P. *Macromolecules* **1993**, *26*, 5336.
(10) Boiko, Y. M.; Prud'homme, R. E. *J. Appl. Polym. Sci.* **1999**, *74*, 825.
(11) Sha, Y.; Hui, C. Y.; Ruina, A.; Kramer, E. J. *Macromolecules* **1995**, *28*, 2450.
(12) Schnell, R.; Stamm, M.; Creton, C. *Macromolecules* **1998**, *31*, 2284.
(13) Ezekoye, O. A.; C. D., L.; Fahey, M. T.; Hulme-Lowe, A. G. *Polym. Eng. Sci.* **1998**, *38*, 976.
(14) Jonza, J. M.; Porter, R. S. *Macromolecules* **1986**, *19*, 1946.
(15) Cheung, Y. W.; Stein, R. S. *Macromolecules* **1994**, *27*, 2512.

(16) Xue, Y.-Q.; Tervoort, T. A.; Rastogi, S.; Lemstra, P. J. *Macromolecules* **2000**, *33*, 7084.
(17) Plummer, C. J. G.; Kausch, H.-H.; Creton, C.; Kalb, F.; Leger, L. *Macromolecules* **1998**, *31*, 6164.
(18) Laurens, C.; Ober, R.; Creton, C.; Leger, L. *Macromolecules* **2001**, *34*, 2932.
(19) McSwain, R. L.; Markowitz, A. R.; Shull, K. R. *J. Polym. Sci., Part B: Polym. Phys.* **2004**, *42*, 3809.
(20) Kuo, S.-W.; Huang, W.-J.; Huang, C.-F.; Chan, S.-C.; Chang, F.-C. *Macromolecules* **2004**, *37*, 4164.
(21) Kim, E.; Kramer, E. J.; Osby, J. O. *Macromolecules* **1995**, *28*, 1979.
(22) Katana, G.; Kremer, F.; Fischer, E. W.; Plaetschke, R. *Macromolecules* **1993**, *26*, 3075.
(23) Shull, K. R.; Ahn, D.; Chen, W.-L.; Flanigan, C. M.; Crosby, A. J. *Macromol. Chem. Phys.* **1998**, *199*, 489.
(24) Shull, K. R. *Mater. Sci. Eng., R* **2002**, *R36*, 1.
(25) Ahn, D.; Shull, K. R. *Langmuir* **1998**, *14*, 3637.
(26) Ahn, D.; Shull, K. R. *Langmuir* **1998**, *14*, 3646.
(27) Crosby, A. J.; Shull, K. R.; Lakrout, H.; Creton, C. *J. Appl. Phys.* **2000**, *88*, 2956.
(28) Ahn, D.; Shull, K. R. *Macromolecules* **1996**, *29*, 4381.
(29) Barquins, M.; Maugis, D. *J. Adhes.* **1981**, *13*, 53.
(30) Massoud, H. Z.; Plummer, J. D.; Irene, E. A. *J. Electrochem. Soc.* **1985**, *132*, 2685.
(31) Deal, B. E.; Grove, A. S. *J. Appl. Phys.* **1965**, *36*, 3770.
(32) Tsuburaya, M.; Saito, H. *Polymer* **2004**, *45*, 1027.
(33) Brus, J.; Dybal, J.; Schmidt, P.; Kratochvil, J.; Baldrian, J. *Macromolecules* **2000**, *33*, 6448.
(34) Li, C.; Kong, Q.; Fan, Q.; Xia, Y. *Mater. Lett.* **2005**, *59*, 773.
(35) Lodge, T. P.; Wood, E. R.; Haley, J. C. *J. Polym. Sci., Part B: Polym. Phys.* **2005**, *44*, 756.
(36) Lodge, T. P.; McLeish, T. C. B. *Macromolecules* **2000**, *33*, 5278.
(37) Fox, T. G. *Bull. Am. Phys. Soc.* **1956**, *1*, 123.
(38) Hui, C.-Y.; Wu, K.-C.; Lasky, R. J.; Kramer, E. J. *J. Appl. Phys.* **1987**, *61*, 5129.
(39) Hui, C.-Y.; Wu, K.-C.; Lasky, R. J.; Kramer, E. J. *J. Appl. Phys.* **1987**, *61*, 5137.